

# Evaluating earthquake-induced liquefaction in the urban area of Larissa, Greece

George Papathanassiou · Kostas Seggis · Spyros Pavlides

Received: 15 June 2009 / Accepted: 6 March 2010 / Published online: 8 April 2010  
© Springer-Verlag 2010

**Abstract** The paper evaluates the liquefaction potential of the subsoil layers at the town of Larissa (Thessaly Plain, Central Greece). Using data from 53 borings with SPT measurements, the liquefaction potential was evaluated based on simplified procedures and by applying the methodology of the liquefaction potential index to the parameters of the soil columns. Maps were developed indicating the quantitative characteristics of the liquefiable layers and the area where there was a probability of surface evidence of liquefaction. The study indicated that the urban area of Larissa should be considered as a low liquefaction area, with the exception of a few sites close to the River Pinios where the liquefaction potential was characterized as medium to high.

**Keywords** Liquefaction probability · Hazard · Larissa · Greece

**Résumé** L'article évalue le potentiel de liquéfaction de couches du sous-sol de la ville de Larissa (Plaine de Thessalie, Grèce centrale). A partir des données de 53 forages comportant des mesures SPT, le potentiel de liquéfaction a été évalué suivant des procédures simplifiées et en appliquant la méthodologie de l'indice de potentiel de liquéfaction en colonnes de sols. Des cartes ont été établies indiquant les caractéristiques des couches liquéfiables et les surfaces où il y avait une probabilité de liquéfaction. L'étude a conclu que la zone urbaine de Larissa devrait être

considérée comme une région de faible potentiel de liquéfaction, à l'exception de quelques sites près de la rivière Pinios où le potentiel de liquéfaction a été défini comme moyen à élevé.

**Mots clés** Probabilité de liquéfaction · Aléa · Larissa · Grèce

## Introduction

Greece is one of the mostly highly seismic countries in the Mediterranean region. Using Greek Seismic Codes, the earthquake-prone area around the town of Larissa, central Greece, has been assigned a design acceleration on seismic bedrock of 2.4 g. Historical reports of earthquakes and sand boils associated with the earthquake of 1941 indicate that liquefaction has occurred beneath part of Larissa. The town is situated on sediments deposited by the Pinios River hence Larissa could be classified as a liquefaction-prone area. This paper considers the hazard posed by the nature of these soft saturated sediments.

The aim of the study was the evaluation of the liquefaction susceptibility of the subsoil layers and the computation of the probability of liquefaction-induced surface distress in the urban area of Larissa. Geotechnical profiles were prepared based on borings with SPTs and the factors of safety against liquefaction of the soil layers was estimated using published procedures (Youd et al. 2001). The susceptibility to liquefaction of the soil elements was evaluated using the modified criteria by Seed et al. (2003) and the probability of liquefaction manifestation was estimated using the LPI-based regression proposed by Papathanassiou (2008). This approach was used as it is the only model which takes into account the new susceptibility

G. Papathanassiou (✉) · S. Pavlides  
Department of Geology, Aristotle University of Thessaloniki,  
Egnatia str, 54149 Thessaloníki, Greece  
e-mail: gpapatha@auth.gr

K. Seggis  
Mandilara 20, 41222 Larissa, Greece

criteria of Seed et al. (2003). The parameters of the seismic scenario employed in this study were obtained from the Greek Seismic Code, taking into account the effect of surface geology in the evaluation of site amplification.

As a result of this study, quantitative parameters of the liquefiable subsoil layers (such as depth and thickness), were identified and their spatial distribution mapped. The liquefaction potential index (LPI) of the soil columns and the relative probability of liquefaction-induced surface disruption were computed in order to compile a liquefaction hazard map.

Although this study indicates the existence of liquefiable soil layers below the surface, for an earthquake scenario of magnitude M 7.0 and a PGA value of 0.25 g the probability of manifestations of liquefaction at the surface is higher than 50% only at sites close to the River Pinios. In particular, only at two sites in the northern part of the city was the probability >50%—the threshold defined as the boundary between the occurrence and non-occurrence of liquefaction-induced ground disruption.

#### Liquefaction potential index: methodology, modifications and applications

The methodology of the LPI was proposed by Iwasaki et al. (1978; 1982) for evaluating the liquefaction potential of a soil column. The index reflects the thickness of the liquefiable layer, the thickness of the non-liquefiable (cap) layer and the value of the factor of safety against liquefaction. Iwasaki et al. (1982) calibrated the severity of liquefaction-induced damages with the LPI values using data provided by 87 borings with SPT values in liquefied and non-liquefied sites in Japan. According to this calibration, liquefaction failure potential ranges from >15 (extremely high) to 0 (extremely low), i.e. high is between 5 and 15 and low between 0 and 5. The LPI methodology was modified by Sonmez (2003) by adding a threshold value of 1.2 instead of 1 for the factor of safety and by introducing two new categories for the lower values: 0 non-liquefiable; 0–2 low liquefiable and 2 and 5 moderate liquefiable.

Toprak and Holzer (2003) attempted to relate LPI with the severity of the surface manifestations of liquefaction using CPTs from the 1989 Loma Prieta, California, earthquake. They observed that the median values of LPI were 5 and 12 respectively in areas where sand boils and lateral spreads occurred. Lower and upper quartiles were 3 and 10 for sand boils and 5 and 17 for lateral spreads (Holzer 2008). Recently, Papathanassiou (2008) proposed a new calibration that resulted from the application of the box-whisker plot method to the SPT data. His study indicated that at sites where  $\text{LPI} > 32$  liquefaction-induced failures classified as “high” (such as lateral spreading phenomena) are likely to occur, while at sites where  $\text{LPI} < 19$  no liquefaction

manifestations would be expected. Where the LPI value ranged between 19 and 29, a “medium” degree of liquefaction manifestation (such as sand boils and ejection of material) would be likely to occur. Papathanassiou (2008) explained the differences from the threshold LPI proposed by Iwasaki et al. (1982), Toprak and Holzer (2003) by the fact that in his study the evaluation of liquefaction susceptibility of soil layers was based on the modified criteria proposed by Seed et al. (2003) rather than the ones suggested by Wang (1979) known as the “Chinese criteria”.

Lee et al. (2003) re-calibrated the scale based on CPT data from liquefied sites in Taiwan associated with the 1999 Chi-Chi earthquake. They proposed that the liquefaction potential of a site is very high where LPI is >30 and low where it <20, with medium potential where the LPI values range between 20 and 30. Sonmez and Gokceoglu (2005) proposed a new classification using the probability of liquefaction (PL) in lieu of the factor of safety in order to compute the LPI or Liquefaction Severity Index (Ls) as they called it in their paper. Furthermore, Li et al. (2006) defined the LPI or IL as a function of the probability of liquefaction and proposed mathematical formulae for the evaluation of the probability of liquefaction-induced ground failure. Finally, Papathanassiou (2008), using a logistic regression analyses, proposed a LPI-based approach for the calculation of the probability of liquefaction manifestations. For a comprehensive description of these procedures, the reader is referred to Holzer (2008).

The advantage of LPI is that it quantifies the likelihood of liquefaction at the site by providing a unique value for the entire soil column instead of factors of safety for each of the layers. Consequently, the LPI values were used for the compilation of liquefaction hazard maps which can be used by planners as a tool for the preliminary assessment of the liquefaction potential. Such thematic maps were published for Evansville, USA (Kayabali and West 1994), for Puerto Rico, USA by Divakarla et al. (1998), for Busehr, Iran (Hosseini 1998), for Treasure Island, USA by Luna and Frost (1998), for the Romagna coast in Italy by Crespanelli et al. (1999), for the state of California, USA (Holzer et al. 2002), for the town of Inegol, Turkey (Sonmez 2003; Sonmez and Gokceoglu 2005), for the town of Ceyhan, Turkey (Ulusay and Kuru 2004), for the city of Lefkada, Greece (Papathanassiou et al. 2005), for Memphis, USA (Rix and Romero-Hudock 2007), Charleston, USA by Hayati and Andrus (2007) and Juang and Li (2007), California, USA by Lenz and Baise (2007) and Memphis, USA (Cramer et al. 2008).

#### Geology of the area

The Larissa Basin is one of the main graben of the Internal Hellenides that were created by NE–SW crustal trenching

during the Late Miocene-Pliocene (Caputo et al. 2004). It crosses the Tyrnavos Basin which is bordered by a number of active faults: the Rodia (RF) and Gyrtoni (GF) to the north; the Tyrnavos (TF) and Larissa (LF) faults to the south and the Asmaki (AF), Omolio (OF) and Ligaria (IF); see Fig. 1. These E–W and ESE–WNW faults occurred as an extensional phase began during the Middle to Late Pleistocene (Caputo and Pavlides 1993). The recent seismicity of Northern Thessaly shows that this extensional regimen is still active (Caputo et al. 2004).

Caputo and Pavlides (1993) concluded that the Larissa Basin is an alluvial plain formed by Quaternary deposits in stratigraphic continuity with the Pliocene sediments. Deposits of Pliocene age outcrop on the northern border of the Larissa Basin near Rodia where they appear to overlie Palaeozoic/Mesozoic substrata. Caputo and Pavlides (1993) also note that Red Beds outcrop locally along the borders of the basin. The maximum thickness of the lacustrine deposits and overlying conglomerates has been estimated as 500 m. The town of Larissa itself is built on Recent alluvial deposits in the plain, on man-made deposits consisting of embankments/artificial fills and on strata of Neogene age.

## Historical seismicity

The eastern part of the Thessaly region can be divided into two parts as regards the occurrence of earthquakes. The southern part was ruptured by strong earthquakes during the twentieth century after an apparent quiescence since 1773 while the northern part, including the town of Larissa, experienced seismicity in 1941 (Caputo and Helly 2005). Papadopoulos (1992) has suggested the apparent quiescence during the 1800s is likely to be related to changing

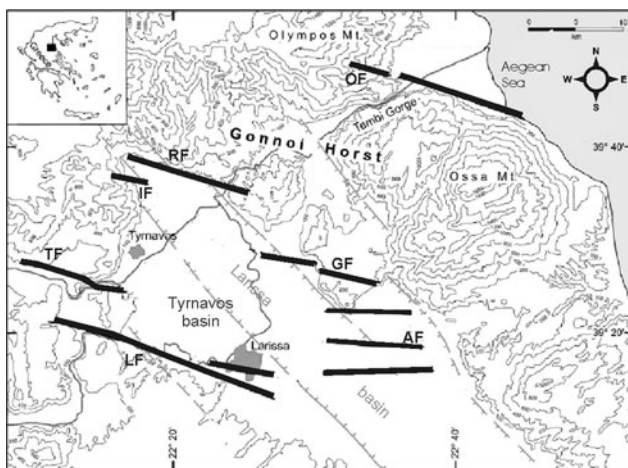


**Fig. 1** Major tectonic structures at the area of Larissa basin (from Caputo et al. 2004)

seismicity patterns rather than an incomplete earthquake record.

Data regarding the 12 historical seismic events in Thessaly (Table 1) and the earthquake parameters were obtained from the seismic catalogues of Papazachos and Papazachou (1997) and Papazachos et al. (2007), respectively (Fig. 2). As seen in Table 1, six events occurred in the northern region from 1668 to 1941 while six events with a magnitude  $>6.0$  occurred in the southern part of Thessaly during the twentieth century.

The secondary effects triggered by the earthquakes are described in historical seismicity catalogues.

- The 1731 earthquake caused the collapse of 10 houses and mosques in the city of Larissa
- The 1766 event, as described in a chronicle of the monastery of Panagia Olympiotissa, triggered severe structural damage.
- The 28 August 1781 earthquake caused casualties and damage to houses and mosques which was exacerbated by the fire triggered by the shock.
- The 9 January 1892 earthquake was the most severe event during the nineteenth century, causing severe structural damage in Larissa although the epicenter was some 10 km to the NE of the city (Papaioannou 1981).
- The March 1941 earthquake was the strongest to occur close to the town of Larissa during the twentieth century, triggering many secondary effects such as ground cracks, liquefaction and subsidence. Maravelakis (1943) noted the event caused structural damage to the villages of Gerakari, Eleftherio, Nesson, Orta, Nehali, Platikampos, Glafki ad Halki. In Larissa, structural damage was reported in the industrial area

**Table 1** Historical seismicity of eastern Thessaly region

| Date             | Lat.  | Long. | M   |
|------------------|-------|-------|-----|
| Northern part    |       |       |     |
| 1668             | 39.65 | 22.3  | 6.3 |
| 1731             | 39.7  | 22.3  | 6.0 |
| 9 November 1766  | 39.8  | 22.2  | 6.3 |
| 28 August 1781   | 39.65 | 22.4  | 6.4 |
| 22 January 1892  | 39.7  | 22.55 | 6.0 |
| 1 March 1941     | 39.7  | 22.54 | 6.3 |
| Southern part    |       |       |     |
| 20 January 1905  | 39.67 | 22.83 | 6.6 |
| 23 February 1930 | 39.6  | 23.1  | 6.0 |
| 30 April 1954    | 39.22 | 22.28 | 6.7 |
| 19 April 1955    | 39.3  | 23.03 | 6.2 |
| 8 March 1957     | 39.36 | 22.63 | 6.6 |
| 9 July 1980      | 39.23 | 22.76 | 6.4 |

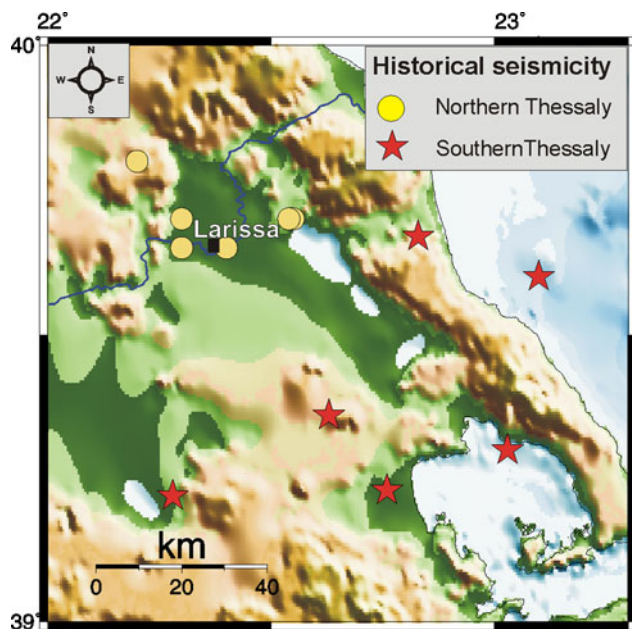


**Fig. 2** Distribution of historical seismicity in the region of eastern Thessaly

of Tabakika, at the centre of the city and in the area around the castle. This author evaluated intensity as IX of the Mercalli-Sieberg scale while Galanopoulos (1981) evaluated the intensity as VIII.

Maravelakis (1943) recorded a 12 km SE–NW surface rupture and some subsidiary parallel cracks. At the same time, along the River Pinios and its tributaries the ground slumped and for many kilometers cracks appeared along the banks. Liquefaction phenomena were reported from many places within the town together with the development of high artesian pressures that resulted in damage to deep wells.

In addition, at the village of Eleftherion, water was ejected from a well, sand volcanoes were observed on the banks of River Mirou, and water ejection was observed at many places in the village of Nesson. Furthermore, slope failures occurred in the River Pinios embankments while ground cracks opened in the lower slopes of the castle mound, with structural damage experienced in nearby buildings as well as the castle at the top of the hill (Maravelakis 1943).

### Subsoil characteristics

In order to define the properties of the subsoil layers, 53 boreholes, 10–15 m deep with SPT measurements were evaluated. The SPT-N values, the grain size distribution, the liquid limit and the plasticity index of selected samples were also included in the geotechnical profiles. The

locations of the borings are shown in Fig. 3 and the line of cross-sections A–A' and B–B', the details of which are given in Fig. 4.

At Larissa the upper layer generally consists of an artificial fill with an average thickness of 2 m, although in some sites it reaches 4 m. This layer of fill consists mainly of clay, sand, sandy gravels and material from construction sites. Beneath this upper layer the subsoil is characterized by clayey and sandy formations deposited by the River Pinios. The main characteristic of these fluvial deposits is the vertical and horizontal heterogeneity due to the seasonal fluctuations of the River Pinios.

As shown in the cross-section A–A', in the north west (BH 43) beneath the artificial fill there is a thin (2 m) silty soil with SPT-N values of 10 overlying 6 m of sandy material with  $N$  values >30. Thicker sandy layers, classified as non-plastic SM soils, were also present in BHs 29 and 9, where the  $N$  values ranged from 8 to 12. Towards the south east, clayey layers were encountered in BHs 4 and 34 with thicknesses of some 6 m and  $N$  values from 18 to 22. These layers were classified as high plasticity clays as their liquid limit and plasticity indices were 72 and 52% (BH 4) and 65 and 43% (BH 34).

The heterogeneity of the subsoil formation at Larissa is also presented in cross-section B–B' (Fig. 4). As seen in the figure, on the western side (BH 47), beneath the artificial cap layer is a 9 m thick clayey stratum. The SPT-N values range from 27 to 41 with an average of 31. This generally CL layer is interrupted by a SC layer with 30% fines in which the liquid limit and plasticity index are 19 and 4% respectively and the  $N$  value is 29. Moving eastwards, the stratum becomes sandy, particularly in BHs 18, 6 and 5. The thickness of this stratum varies from 4 m (BH 18) to 8 m (BH 5). The  $N$  values range between 14 and 20 in BHs 5 and 6 respectively but increase to 32 in the silty

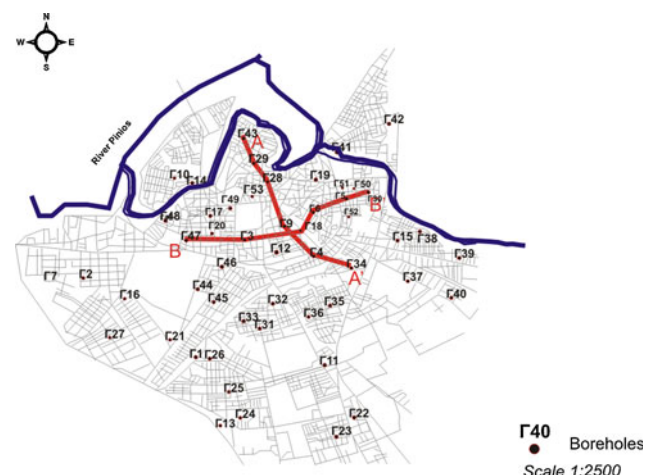


**Fig. 3** Map showing the locations of boreholes and the surface traces of cross-sections A–A' and B–B'

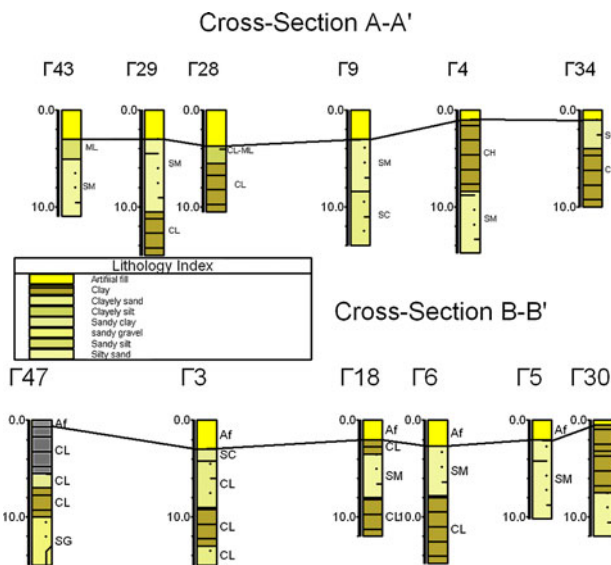


**Fig. 4** Cross-sections A–A' and B–B'

sand layer in BH 18. Finally, in BH 30 the SM stratum lies beneath a 6 m thick CL layer and as a consequence the SPT  $N$  values are 4–6 near the surface rising to 22–24 at depth. The non-plastic SM stratum has an average  $N$  value of 22 and 8% fines while the CL soil has an average of 85% fines.

### Evaluating the susceptibility to liquefaction of the subsoil layers

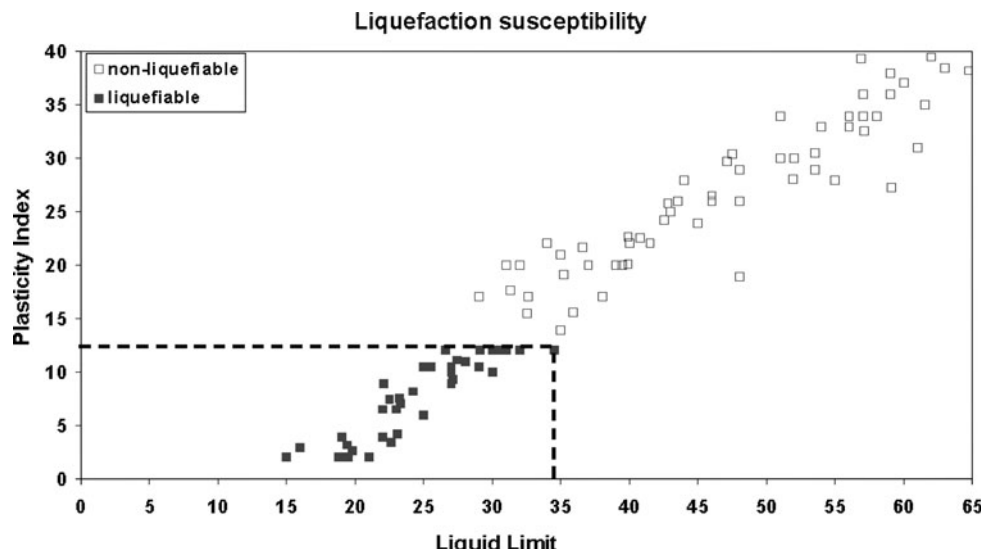
In the past, the evaluation of the liquefaction susceptibility of a soil layer was achieved by applying the “Chinese” criteria (Wang 1979) or the guidelines proposed by

Andrews and Martin (2000). Both of these criteria take into account the presence of a fine grained material in the soil element and particularly of a percentage of clay size. However, papers published by Seed et al. (2003) and Bray and Sancio (2006) stated that the plasticity behavior of fine grained particles of soils is more important than the clay-size fraction. Thus, they proposed new criteria where soils with a fines content >35% are considered as potentially liquefiable when the liquid limit is <37%, the plasticity index <12% and the water content is high relative to the liquid limit (Seed et al. 2003).

In this study, the liquefaction susceptibility of the subsoil in the urban area of Larissa was screened based on the modified criteria proposed by Seed et al. (2003) which were applied to the data provided by the geotechnical profiles of 53 boreholes with SPT measurements. The majority of these borings were drilled by the private company of Georesearch GP, Larissa, and some as part of a study performed by Tsotsos and Pitilakis (1995). It can be seen from Fig. 5 that there is a clear distinction between those soils which will liquefy and those which are unlikely to liquefy, on their liquid limit and plasticity index. The majority of the non-liquefiable soils have values of up to 60% LL and 40% PI.

Figure 6 shows the susceptibility to liquefaction along the cross-sections (A–A' and B–B') identified in Fig. 3. Beneath the non-liquefiable cap layer the sandy stratum is characterized as susceptible to liquefaction material while the clayey material is non-liquefiable. The thickness of the liquefiable stratum ranges from 2 m (BH 28) to 9 m (BH 29) while the non-liquefiable layer also has a thickness of up to 9 m. Regarding the cross-section B–B', the liquefiable stratum has been mapped in every borehole, with a thickness of up to 6 m in BH 6.

**Fig. 5** Liquefaction susceptibility of soil layers based on their Atterberg limits



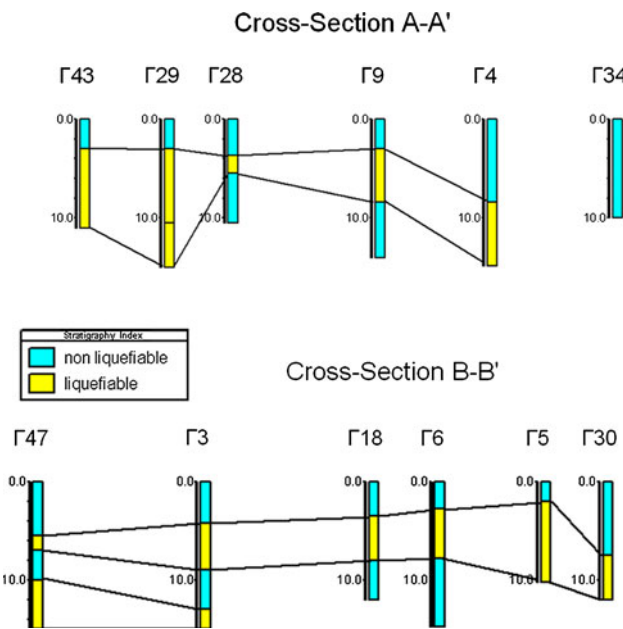


**Fig. 6** Cross-sections A–A' and B–B' with respect to liquefaction susceptibility of the soil layers

### Evaluation of the liquefaction potential in the urban area of Larissa

Usually, the liquefaction potential of a soil layer is computed based on the deterministic simplified procedure proposed by Seed and Idriss (1971) and the modifications to this procedure published later by Seed et al. (1985) and Youd et al. (2001). According to these recommendations, the factor of safety against liquefaction of a soil layer ( $f_s$ ) triggered by a seismic event is defined as the ratio of cyclic resistance ratio (CRR) over cyclic stress ratio (CSR). The former is a function of the in situ test data such as the SPT-N values and the latter a function of the parameters of the earthquake represented by the magnitude ( $M$ ) and the peak ground acceleration (PGA).

#### Defining the earthquake parameters used

In this study, the seismic parameters suggested by the Greek Earthquake Planning and Protection Organization (EAK 2000) were initially taken into account in order to calculate the CSR. According to these recommendations, in the area of Larissa the design acceleration is 0.24 g for rock outcrop conditions, with a 10% probability (Pt) of being exceeded over a period (t) of 50 years. The return period for this PGA value, computed as a function of Pt and t, is equal to  $T = 475$  years, while the maximum earthquake magnitude for the same recurrence interval is  $M = 7$  (Papazachos and Papazachou 1997). However, as much of the city of Larissa is built on fluvial sediments, it was

decided to investigate the influence of the near-surface geology on the final acceleration value.

In order to account for amplification effect due to surface geology, the regression proposed by Stewart et al. (2003) was used. As the sediments forming the Larissa plain are generally Holocene alluvial deposits and Stewart et al. (2003) suggest Holocene alluvial deposits are classified as Quaternary alluvium (Qa), this classification was used for all the deposits.

The amplification factor ( $f$ ) and the surface acceleration  $a_{\max}$  were computed using the equations proposed by Stewart et al. (2003):

$$\ln(f) = a + b \ln(\text{PGA}) a \quad (1)$$

$$a_{\max} = \text{PGA} * f \quad (2)$$

where  $f$  is the amplification factor;  $a$ , and  $b$  are parameters depending on the age of the material and texture of soil; PGA is the value of design acceleration for rock outcrop conditions;  $a_{\max}$  is the value of surface acceleration used for the evaluation of liquefaction potential.

The values of  $a$  and  $b$  used were  $-0.15$  and  $-0.13$  for the Qa classification and the calculated  $a_{\max}$  value was  $0.25$  g.

Thus, the parameters of the seismic “loading” used for the calculation of CSR were  $M = 7.0$  (earthquake magnitude corresponding to 475-year return period) and  $a_{\max} = 0.25$  g for the Qa soil conditions.

The CSR is expressed as:

$$\text{CSR} = 0.65 \times \left( \frac{a_{\max}}{g} \right) \times \left( \frac{\sigma_{vo}}{\sigma'_{vo}} \right) \times r_d \quad (3)$$

where  $\sigma_{vo}$ : total vertical stress at depth  $z$ ;  $\sigma'_{vo}$ : effective vertical stress at the same depth;  $a_{\max}$ : peak horizontal ground acceleration;  $g$ : acceleration due to gravity; and  $r_d$ : stress reduction factor. In this study, the term  $r_d$  was estimated using the Liao and Whitman (1986) equation:

$$r_d = 1.0 - 0.00765 \times z \quad \text{for } z \leq 9.15 \text{ m} \quad (4)$$

$$r_d = 1.174 - 0.0267 \times z \quad \text{for } 9.15 \text{ m} < z < 23 \text{ m}. \quad (5)$$

The CSR values were divided by the magnitude scaling factor (MSF) which is calculated by the following equation, Youd et al. (2001):

$$\text{MSF} = \left( \frac{M_w}{7.5} \right)^{2.56} \quad (6)$$

and the CRR was computed using the following equation (Youd et al. 2001)

$$\text{CRR} = \frac{1}{34 - N_{1(60)}} + \frac{N_{1(60)}}{135} + \frac{50}{[10 \times N_{1(60)} + 45]^2} - \frac{1}{200} \quad (7)$$

The calculation of  $N_{1(60)}$  is influenced by the measured standard penetration resistance  $N$ ; the overburden pressure

**Table 2** Quantitative parameters of the subsoil layers regarding liquefaction potential

| Borehole | Thickness of cap layer (m) | Thickness of liquefiable stratum (m) | Probability of liquefaction surface manifestation (%) | LPI   |
|----------|----------------------------|--------------------------------------|---|-------|
| g1       | 10                         | 0                                    | 4.34  | 0     |
| g2       | 10                         | 0                                    | 4.34  | 0     |
| g3       | 10                         | 0                                    | 4.34  | 0     |
| g4       | 10                         | 0                                    | 4.34  | 0     |
| g5       | 10                         | 0                                    | 4.34  | 0     |
| g6       | 3.5                        | 3                                    | 8.61  | 3.35  |
| g7       | 10                         | 0                                    | 4.34  | 0     |
| g8       | 10                         | 0                                    | 4.34  | 0     |
| g9       | 3                          | 5.4                                  | 68.51   | 17.75 |
| g10      | 10                         | 0                                    | 4.34  | 0     |
| g11      | 10                         | 0                                    | 4.34  | 0     |
| g12      | 10                         | 0                                    | 4.34  | 0     |
| g13      | 10                         | 0                                    | 4.34  | 0     |
| g14      | 3                          | 2.5                                  | 6.48  | 1.94  |
| g15      | 10                         | 0                                    | 4.34  | 0     |
| g16      | 10                         | 0                                    | 4.34  | 0     |
| g17      | 10                         | 0                                    | 4.34  | 0     |
| g18      | 10                         | 0                                    | 4.34  | 0     |
| g19      | 10                         | 0                                    | 4.34  | 0     |
| g20      | 10                         | 0                                    | 4.34  | 0     |
| g21      | 10                         | 0                                    | 4.34  | 0     |
| g22      | 10                         | 0                                    | 4.34  | 0     |
| g23      | 10                         | 0                                    | 4.34  | 0     |
| g24      | 10                         | 0                                    | 4.34  | 0     |
| g25      | 10                         | 0                                    | 4.34  | 0     |
| g26      | 10                         | 0                                    | 4.34  | 0     |
| g27      | 10                         | 0                                    | 4.34  | 0     |
| g28      | 3                          | 2.5                                  | 8.24  | 3.13  |
| g29      | 3                          | 10                                   | 13.34   | 5.6   |
| g30      | 7                          | 6                                    | 22.42   | 8.49  |
| g31      | 10                         | 0                                    | 4.34  | 0     |
| g32      | 10                         | 0                                    | 4.34  | 0     |
| g33      | 10                         | 0                                    | 4.34  | 0     |
| g34      | 10                         | 0                                    | 4.34  | 0     |
| g35      | 10                         | 0                                    | 4.34  | 0     |
| g36      | 10                         | 0                                    | 4.34  | 0     |
| g37      | 7                          | 4.5                                  | 6.56  | 2     |
| g38      | 10                         | 0                                    | 4.34  | 0     |
| g39      | 10                         | 0                                    | 4.34  | 0     |
| g40      | 10                         | 0                                    | 4.34  | 0     |
| g41      | 10                         | 0                                    | 4.34  | 0     |
| g42      | 10                         | 0                                    | 4.34  | 0     |
| g43      | 10                         | 0                                    | 18.00   | 7.23  |
| g44      | 9                          | 2                                    | 5.75  | 1.36  |
| g45      | 10                         | 0                                    | 4.34  | 0     |
| g46      | 10                         | 0                                    | 4.34  | 0     |
| g47      | 10                         | 0                                    | 4.34  | 0     |
| g48      | 10                         | 0                                    | 4.34  | 0     |
| g49      | 3                          | 6                                    | 81.57   | 21    |
| g50      | 4.5                        | 4.5                                  | 12.65   | 5.32  |
| g51      | 10                         | 0                                    | 4.34  | 0     |
| g52      | 10                         | 0                                    | 4.34  | 0     |
| g53      | 10                         | 0                                    | 4.34  | 0     |

factor  $C_n$ ; the correction for hammer energy ratio (ER)  $C_e$ ; the correction for borehole diameter,  $C_b$ ; the correction factor for rod length  $C_r$ ; and the correction for samplers with or without liners. The  $C_n$  was calculated according to the equation proposed by Liao and Whitman (1986),  $C_n = (P_a/\sigma_{vo})^{0.5}$  while the others factors were estimated using the parameters suggested by Youd et al. (2001). Additionally, a “fine content” correction was applied to the calculated  $N_{1(60)}$  value in order to obtain an equivalent clean sand value  $N_{1(60)cs}$  given by the equations proposed by Youd et al. (2001).

#### Quantitative characteristics of the liquefaction-prone subsoil layers

Having computed the CRR of the soil layers and the CSR regarding the earthquake “scenario”, the factor of safety against liquefaction was calculated. Afterwards, the depth and the thickness of the liquefied layers per borehole were defined based on the computed values of  $f_s$  of the soil layers (Table 2).

The depth of the liquefiable layer is evaluated by taking into account the depth of the upper subsoil layer susceptible to liquefaction, for which the factor of safety was estimated as less than one ( $f_s < 1$ ). The evaluated thickness of the liquefiable layers in a borehole represents the

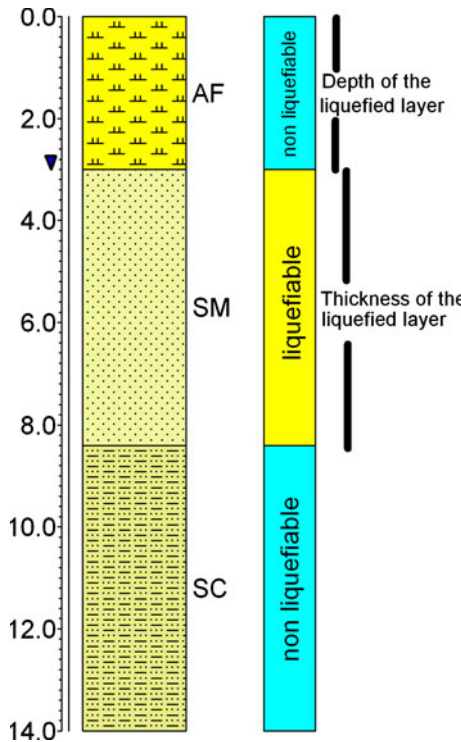


**Fig. 7** Quantitative characteristics of the liquefiable stratum in borehole BH 9

cumulative thickness of the liquefiable horizons (see BH 9, Figs. 7, 8).

The thicker liquefiable stratum reaches 9 m in BH 29 while the liquefiable layer closest to the ground surface was located in BHs 9, 14, 28, 29 and 49 (3 m). However, in most cases, the soil elements that were classified as susceptible to liquefaction using the criteria proposed by Seed et al. (2003) were evaluated as non-liquefiable ( $f_s > 1$ ) due to the high percentage of fines within the soil elements and the fact that the  $N$  value in most of the soil layers was  $>20$ , indicating a relatively dense soil. In particular, soil strata characterized as prone to liquefaction under this specific seismic loading were identified in only 9 of the 53 boreholes (9, 14, 28, 29, 30, 37, 44, 49 and 50; see Fig. 8).

#### Assessment of the probability of liquefaction-induced ground disruption

Varnes (1984) defined natural hazard as the probability of occurrence of a potentially damaging phenomenon within

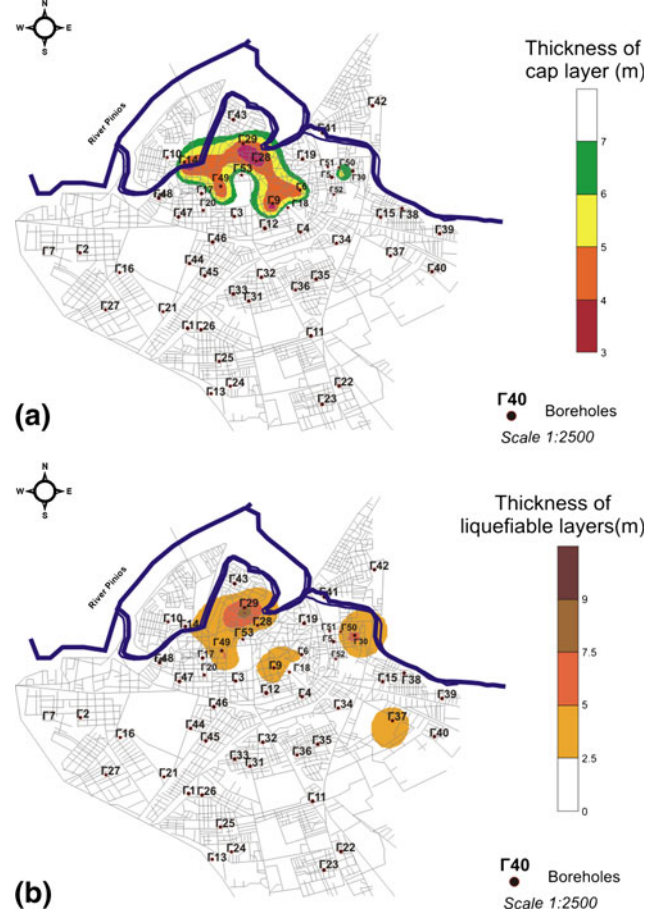


**Fig. 8** Maps compiled based on **a** the spatial distribution of the thicknesses of the cap layer and **b** the liquefiable strata

a given area and in a given period of time. The aim of the present study was therefore the assessment of liquefaction hazard and the compilation of a map showing spatially the probability of liquefaction-induced surface disruption. To achieve this, the LPI of each borehole was calculated using the methodology proposed by Iwasaki et al. (1982).

$$\text{LPI} = \int_0^z F(z)W(z)dz \quad (8)$$

where  $z$  is the depth below the ground surface in meters, calculated as  $W(z) = 10 - 0.5z$ ;  $F(z)$  is a function of the factor of safety against liquefaction  $f_s$ , where  $F(z) = 1 - f_s$  when  $f_s < 1$  and if  $f_s > 1$  then  $F(z) = 0$ .

The index is related to the thickness of the liquefiable layer, the thickness of the non-liquefiable cap layer and the factor of safety against liquefaction. In each borehole, only the soil layers which both had an  $f_s < 1$  and satisfied the liquefaction susceptibility criteria [based on Seed et al. (2003) modified criteria] were taken into account for the calculation of the LPI. The computation of LPI was accomplished using the software LiqIT v 4.7 (2006).

The computed values of LPI at each location were used in the equation proposed by Papathanassiou (2008) for evaluating the probability of liquefaction-induced ground disruption:

$$\text{Prob(liquefaction)} = \left( \frac{1}{1 + e^{-(3.092 + 0.218 \times \text{LPI})}} \right) \quad (9)$$

This equation was defined by applying the statistical approach of logistic regression to a dataset taken from records from post earthquake in situ tests in Turkey, Taiwan and Greece. In this model, the LPI value is the independent variable and the occurrence or not of liquefaction phenomena is the dependent variable. At sites where the Prob (liquefaction) is  $\geq 0.5$ , liquefaction phenomena can be expected while non-occurrence of liquefaction is predicted where Prob  $< 0.5$ .

Figure 9 shows the probability of liquefaction-induced ground failure is very low at the town of Larissa, with the computed value of probability  $> 50\%$  at only two sites, close to the River Pinios (67% in BH 9 and 81% in BH 49; see Table 2). At these sites, surface evident of liquefaction is likely with an earthquake of magnitude 7 or more and a surface acceleration of 0.25 g.

## Conclusions

The town of Larissa in Central Greece is in an area of medium seismicity where the design acceleration provided by the Greek Seismic Code is 0.24 g on bedrock and there

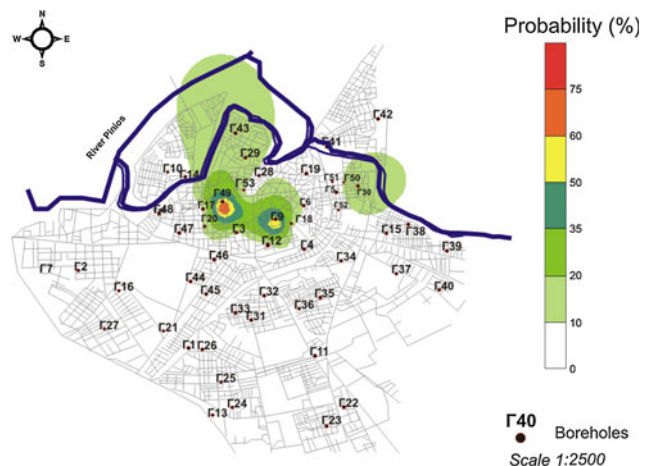


**Fig. 9** Spatial distribution of the probability of liquefaction surface manifestation

is a 10% probability ( $P_t$ ) of this being exceeded in a 50 year period.

The study indicated that deposits susceptible to liquefaction are present in the urban area of Larissa hence a detailed investigation was undertaken based on data from borings with SPT values. The computation showed that taking the Greek Seismic Code earthquake magnitude of 7.0 and 0.25 g acceleration related to the local geological conditions, liquefaction is likely to occur in only two areas close to the River Pinios. This unexpected result could be explained by the fact that the average depth of the groundwater table is  $> 4$  m and the majority of layers susceptible to liquefaction (having an SPT-N  $> 25$ ) are not loose enough to liquefy under this seismic scenario.

**Acknowledgments** The authors would like to thank Mr. Papaioannou for providing information on the historical seismicity of the area.

## References

- Andrews DCA, Martin GR (2000) Criteria for liquefaction of silty soils. In: Proceedings of 12th world conference on earthquake engineering, Upper Hutt, New Zealand, NZ society for earthquake engineering, paper no. 0312
- Bray J, Sancio R (2006) Assessment of the liquefaction susceptibility of fine-grained soils. *J Geotech Geoenviron Eng* 132(9):1165–1177
- Caputo R, Helly B (2005) The Holocene activity of Rodia Fault, Central Greece. *J Geodyn* 40:153–169
- Caputo R, Pavlides S (1993) Late Cainozoic geodynamic evolution of Thessaly and surroundings (central-northern Greece). *Tectonophysics* 223:339–362
- Caputo R, Helly B, Pavlides S, Papadopoulos G (2004) Palaeoseismological investigation of the Tyrnavos Fault (Thessaly, Central Greece). *Tectonophysics* 394:1–20
- Cramer CH, Rix GJ, Tucker K (2008) Probabilistic liquefaction hazard maps for Memphis, Tennessee. *Seismol Res Lett* 78 (in press)

- Crespanelli T, Madiai C, Vannucchi G (1999) Zoning for liquefaction risk in an Italian coastal town using CPT. *Earthquake Geotechnical Engineering*, A. A. Balkema, Rotterdam, pp 561–566
- Divakarla PK, Hoyos LR Jr, Macari EJ (1998) Assessment of liquefaction potential of western Puerto Rico. In: Proceedings of 3rd geotechnical earthquake engineering and soil dynamics conference. ASCE, Reston, pp 530–541
- EAK (2000) Greek seismic code. Earthquake planning and protection organization, Athens, Greece, pp 72 and 7 Appendices (in Greek)
- Galanopoulos GA (1981) The damaging shocks and the earthquake potential of Greece. *Ann Geol Pays Hell* 30:648–724
- Hayati H, Andrus R (2007) Liquefaction potential map of Charleston, South Carolina, based on the 1886 earthquake. Final report to the US Geological Survey (06HQGR0058)
- Holzer TL (2008) Probabilistic liquefaction hazard mapping. *Geotech Earthq Eng Soil Dyn IV*, GSP 181, ASCE
- Holzer TL, Bennett MJ, Noce TE, Padovani AC, Tinsley JC III (2002) Liquefaction hazard and shaking amplification maps of Alameda, Berkeley, Emeryville, Oakland, and Piedmont: a digital database. Open-file report 02-296, US Geological Survey, Menlo Park
- Hosseini SMMM (1998) Microzonation for liquefaction in Busehr, Iran. In: Proceedings of 11th European conference on earthquake engineering. (CD-ROM), A.A. Balkema, Rotterdam
- Iwasaki T, Tatsuoka F, Tokida K-i, Yasuda S (1978) A practical method for assessing soil liquefaction potential based on case studies at various sites in Japan. In: Proceedings of 2nd international conference on microzonation, pp 885–896
- Iwasaki T, Tokida K, Tatsuoka F, Watanabe S, Yasuda S, Sato H (1982) Microzonation for soil liquefaction potential using simplified methods. In: Proceedings of the 3rd international conference on microzonation. 3:1310–1330
- Juang CH, Li DK (2007) Assessment of liquefaction hazard in Charleston Quadrangle, South Carolina. *Eng Geol* 92:59–72. doi: [10.1016/j.enggeo.2007.03.003](https://doi.org/10.1016/j.enggeo.2007.03.003)
- Kayabali K, West TR (1994) Liquefaction susceptibility evaluation for the City of Evansville, Indiana. *Bull Assoc Eng Geol* 31(2):231–253
- Lee D-H, Ku C-S, Yuan H (2003) A study of the liquefaction risk potential at Yuanlin, Taiwan. *Eng Geol* 71(1–2):97–117
- Lenz JA, Baise LG (2007) Spatial variability of liquefaction potential in regional mapping using CPT and SPT data. *Soil Dyn Earthq Eng* 27(7):690–702
- Li DK, Juang CH, Andrus RD (2006) Liquefaction potential index: a critical assessment using probability concept. *Taiwan Geotechnical Society. J Geoeng* 1(1):11–24
- Liao S, Whitman RV (1986) Overburden correction factor for SPT in sand. *J Geotech Eng ASCE* 112(3):373–377
- LiqIT 4.7 (2006). Software for the evaluation of the liquefaction potential of soils. GeoLogismiki, Serres Greece
- Luna R, Frost DJ (1998) Spatial liquefaction analysis system. *J Comput Civil Eng* 12(1):48–56
- Maravelakis (1943) Geological and macroseismic study of the devastating earthquake of Larissa, 1 March 1941, p 27
- Papadopoulos G (1992) Rupture zones of strong earthquakes in the Thessalia region, Central Greece. In: Proceedings of the XXIII general assembly ESC Prague. 2:337–370
- Papaioannou (1981) The earthquake of 1892, Larissa. Newspaper “Eleftheria”, 15 March 1981
- Papathanassiou G (2008) LPI-based approach for calibrating the severity of liquefaction-induced failures and for assessing the probability of liquefaction surface evidence. *Eng Geol* 96:94–104
- Papathanassiou G, Pavlides S, Ganias A (2005) The 2003 Lefkada earthquake: field observations and preliminary microzonation map based on liquefaction potential index for the town of Lefkada. *Eng Geol* 82(1):12–31
- Papazachos BC, Papazachou K (1997) The earthquakes of Greece, Ziti Publ, Thessaloniki, 304 p
- Papazachos BC, Comninakis PE, Scordilis EM, Karakassis GF, Papazachos CB (2007) A catalogue of earthquakes in the Mediterranean and surrounding area for the period 1901–2006, Publications of Geophysical Laboratory, University of Thessaloniki
- Rix GJ, Romero-Hudock S (2007) Liquefaction potential mapping in Memphis and Shelby County, Tennessee. Report to US Geological Survey, [http://earthquake.usgs.gov/regional/ceus/products/download/Memphis\\_LPI.pdf](http://earthquake.usgs.gov/regional/ceus/products/download/Memphis_LPI.pdf), 27 p
- Seed HB, Idriss IM (1971) Simplified procedure for evaluation soil liquefaction potential. *J Soil Mech Found Div ASCE* 97:1249–1273
- Seed HB, Tokimatsu K, Harder LF, Chung RM (1985) The influence of SPT procedures in soil liquefaction resistance evaluations. *J Geotech Eng Div ASCE* 111(12):1425–1445
- Seed RB, Cetin KO, Moss RES, Kammerer AM, Wu J, Pestana JM, Riemer MF, Sancio RB, Bray JD, Kayen RE, Faris A (2003) Recent advances in soil liquefaction engineering: a unified and consistent framework. In: Proceedings of the 26th annual ASCE L.A. Geotechnical Spring Seminar, Long Beach, California, 71 p
- Sonmez H (2003) Modification of the liquefaction potential index and liquefaction susceptibility mapping for a liquefaction-prone area (Inegol, Turkey). *Environ Geol* 44(7):862–871
- Sonmez H, Gokceoglu C (2005) A liquefaction severity index suggested for engineering practice. *Environ Geol* 48(1):81–91
- Stewart JP, Liu AH, Choi Y (2003) Amplification factors for spectral acceleration in tectonically active regions. *Bull Seismol Soc Am* 93(1):332–352. doi: [10.1785/0120020049](https://doi.org/10.1785/0120020049)
- Toprak S, Holzer TL (2003) Liquefaction potential index: field assessment. *J Geotech Geoenviron Eng* 129(4):315–322
- Tsotsos S, Pitilakis K (1995) Microzonation study of Larissa. Department of Civil Engineering, AUTH, Greece, 254 p
- Ulusay R, Kuru T (2004) 1998 Adana-Ceyhan (Turkey) earthquake and a preliminary microzonation based on liquefaction potential for Ceyhan Town. *Natural Hazards* 32(1):59–88
- Varnes DJ (1984) Landslide hazard zonation: a review of principal and practice. Commission of Landslide of IAEG, UNESCO. *Nat Hazards* (3):63
- Wang W (1979) Some findings in soil liquefaction, Water Conservancy and Hydroelectric Power Scientific Research Institute, Beijing, China
- Youd TL, Idriss IM, Andrus RD, Arango I, Castro G, Christian JT, Dobry R, Finn WDL, Harder LF, Hynes ME, Ishihara K, Koester JP, Liao SSC, Marcuron III WF, Marti GR, Mitchell JK, Moriwaki Y, Power MS, Robertson PK, Seed RB, Stokoe II KH (2001) Liquefaction resistance of soils: summary report from the 1996 NCEER and 1998 NCEER/NSF workshops on evaluation of liquefaction resistance of soils, *J Geotech Geoenviron Eng ASCE* 127(10):817–833